

Index-Matched Boundary Techniques for the Elimination of Acoustical Resonances

Jack H. Parker*

U.S. Air Force Research Laboratory, Wright-Patterson Air Force Base, Ohio 45433
and

Bradley D. Duncan†

University of Dayton, Dayton, Ohio 45469-0245

We extend the principle of optical index of refraction to apply the concept of acoustical index for transverse acoustical wave propagation in strings. The relationship between acoustical index and mass density of the acoustic material is developed. With this theoretical link established, classic index-matching techniques are explored at acoustical boundaries. Proper selection of boundary interface segments leads to the elimination of resonant vibrational modes that occur in rigidly supported strings, while maintaining the nonresonant vibration response.

Nomenclature

| | | |
|--------------------|---|---|
| A_F | = | amplitude attenuation merit factor |
| A_G | = | nonresonant gain merit factor |
| A_H | = | first harmonic amplitude attenuation merit factor |
| A_T | = | wave amplitude in terminal medium |
| A_0 | = | wave amplitude in launch medium |
| A_1 | = | wave amplitude in transition medium |
| c | = | transverse wave speed (general) |
| c_m | = | speed of sound in acoustical launch medium |
| c_0 | = | characteristic speed of sound in acoustical launch medium |
| F_a | = | force due to mass acceleration |
| F_{damp} | = | damping force |
| F_{drive} | = | driving force of string |
| F_τ | = | force due to string tension |
| f_r | = | fundamental resonance frequency |
| j | = | complex number presentation, $\sqrt{-1}$ |
| k | = | wave vector |
| L | = | length |
| M | = | refractive index transfer matrix |
| MF | = | quadratic merit function |
| n | = | index of refraction (general) |
| n_T | = | index of refraction in terminal medium |
| n_0 | = | index of refraction in launch medium |
| n_1 | = | index of refraction in transition medium |
| Q | = | bandwidth to frequency ratio merit factor |
| R | = | reflectance |
| R_d | = | damping coefficient |
| r | = | reflection coefficient |
| T | = | transmittance |
| t | = | time |
| t_r | = | transmission coefficient |
| y | = | transverse displacement |
| Z_m | = | intrinsic acoustic impedance of transition media |
| Z_0 | = | intrinsic acoustic impedance of launch media |
| λ | = | wavelength |
| ρ_s | = | mass density |
| τ | = | tension |
| ψ | = | displacement |

| | | |
|----------------------|---|-------------------|
| ψ_{peak} | = | peak displacement |
| ω | = | angular frequency |

I. Introduction

THE principles of reflection suppression at multilayer boundary interfaces are well established for transverse optical wave propagation.¹ Relationships defining the optical index of materials have analogous counterparts in transverse acoustical propagation and shed light on boundary impedance matching techniques. Application of optical index to acoustical materials promotes the use of alternative tools in describing and manipulating the behavior of multilayer acoustic interfaces in strings, stretched membranes, and beams. In many optical applications, index-matching techniques and their associated tools lead to the development of thin-film coatings for narrowband interference filters and antireflection coatings. In particular, application of an acoustical index for transverse acoustical wave propagation leads to the design of an antireflection acoustical boundary, which can be related mathematically to index-matched optical coating theory.

The index of refraction for an optical material is defined as the ratio of the speed of light in a vacuum to the speed in the material.² As a velocity ratio, the index of refraction embodies the relative propagation phase delay in the optical medium of interest, compared to that accrued in a vacuum. Similarly, as transverse acoustic waves propagate from one medium to another, velocity changes occur, which result in differential phase delays. Acoustical index conveniently represents the relative velocity changes between two media.

In the establishment of relative velocities, selection of a reference medium is somewhat arbitrary. In optics, the reference chosen is a vacuum.³ For the acoustical case, we will find that developments are simplified by a judicious choice of the propagation medium. As a general interpretation, the speed of sound in dry air at standard temperature and pressure might seem like a proper choice. In many applications, however, the free propagation of the acoustic wave occurs in the initial launch medium. Therefore, we will choose the characteristic speed of the acoustic wave in the launch medium as our reference. We will then find that this choice yields mathematical forms for reflectances at boundaries comparable to those developed for the optical domain.

II. Theory

A. Acoustic Index for String Media

The acoustic index for transverse wave propagation can be defined in terms of relative velocities to be

$$n_m = c_0/c_m \quad (1)$$

where c_0 is the characteristic speed of sound in the initial launch medium and c_m is the speed in any subsequent medium.⁴ Note

Received 27 January 2002; revision received 26 September 2002; accepted for publication 31 October 2002. Copyright © 2002 by the American Institute of Aeronautics and Astronautics, Inc. All rights reserved. Copies of this paper may be made for personal or internal use, on condition that the copier pay the \$10.00 per-copy fee to the Copyright Clearance Center, Inc., 222 Rosewood Drive, Danvers, MA 01923; include the code 0001-1452/03 \$10.00 in correspondence with the CCC.

*Research Engineer, Sensors Directorate, AFRL/SNJT, 3050 C. Street.

†Professor, Electrical and Computer Engineering and Electro-Optics Program, 300.

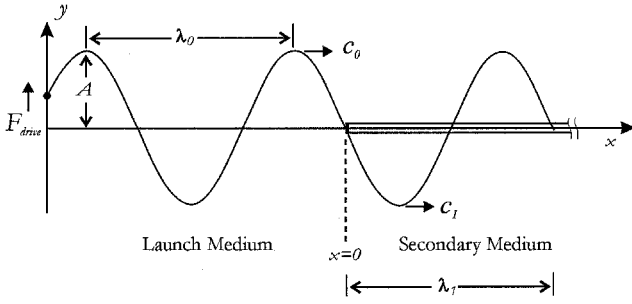


Fig. 1 Transverse wave propagation along a string.

that for transverse propagation, the acoustic index is also related to acoustic impedance by

$$n_m = Z_m / Z_0 \quad (2)$$

where Z_0 and Z_m are the characteristic acoustic impedances of respective media.⁵ To simplify our analysis, we will assume that the acoustic index is not frequency dependent, that is, nondispersive. In all cases, the initial launch medium will be our reference medium in determining other acoustic indices. By Eq. (1) then, the value of the acoustic index of the reference, or initial launch medium, is always $n_0 = 1$ because in this case $c_0 = c_m$.

More specifically, for the case of a tensioned string, the acoustic index can be related to a ratio of mass densities through the relationship

$$n_m = c_0 / c_m = \sqrt{\tau / \rho_0} / \sqrt{\tau / \rho_m} = \sqrt{\rho_m / \rho_0} \quad (3)$$

where τ is the tension, in newtons, and ρ_0 and ρ_m are the mass densities of the launch medium and secondary medium, respectively.⁶

In the case of transverse optical wave propagation, transmission and reflection at optical thin-film interfaces are manipulated in part by properly choosing layers of optical materials with different refractive indices. As we will show later, in the case of transverse acoustic wave propagation in rigidly supported string or membrane structures, Eq. (3) implies that acoustic reflection and transmission can be controlled by carefully tailoring the mass densities of the media at acoustic boundaries.

We now examine the case of a forced vibrating string as shown in Fig. 1 (Ref. 7). The string consists of two media; the initial medium in which the acoustic wave is launched and a secondary medium, of infinite length made of a material having a different mass density than that of the initial medium.

We will assume a driving force in newtons per meter at the left end of the launch medium of the form

$$F_{\text{drive}} = F e^{j\omega t} \quad (4)$$

where ω is the drive frequency in radians per second and F is the amplitude of the driving force. Traveling wave motion is assumed to be in the x direction, with transverse displacements in the y direction given generally as

$$y(x, t) = y_1(ct - x) \quad (5)$$

Motion resulting from the driving force F_{drive} at the driver connection can then be represented in phasor form by $A e^{j\omega t}$, where A is the amplitude of motion along y . We also will define $x = 0$ to be at the media interface so that in the secondary medium we have

$$y_1(0, t) = y_1(c_1 t - 0) = A e^{j\omega t} \quad (6)$$

or

$$y_1(c_1 t) = A e^{jk_1(c_1 t)} \quad (7)$$

where, as in the optics regime, $k_1 = \omega / c_1$ is defined as the wave number. By Eq. (1) we also have that

$$k_1 = n_1 \omega / c_0 \quad (8)$$

where n_1 is the acoustic index of the secondary medium. In addition, because the drive frequency ω is constant in both media and is related to wavelength according to the general relationship⁸

$$\lambda_m \omega = 2\pi c_m \quad (9)$$

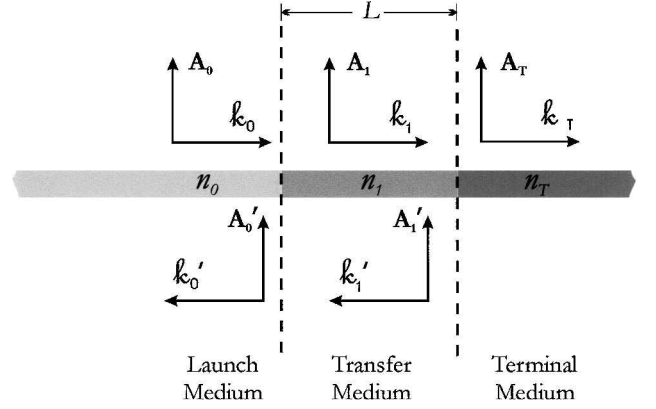


Fig. 2 String with stepped-index boundary.

we find that

$$\omega = 2\pi c_0 / \lambda_0 = 2\pi c_1 / \lambda_1 \quad (10)$$

where λ_0 and λ_1 are the wavelengths in the launch and secondary media, respectively, as shown in Fig. 1. Solving Eq. (10) for λ_1 , we can relate the wavelengths in the two media to acoustic index according to the relationship

$$\lambda_1 = \lambda_0 (c_1 / c_0) = \lambda_0 / n_1 \quad (11)$$

A terminating medium is now added to the end of the string having an acoustic index n_T , as shown in Fig. 2. The change in mass density at each interface causes a portion of the incident wave to be reflected from the boundary, with the remaining portion being transmitted. For our analysis we assume that the interface is lossless with no acoustic absorption present in any of the media. Here the reflected and transmitted transverse waves in each media are represented in vector form: A_0 , A_1 , and A_T are amplitudes of the wave propagating in each medium, each with associated wave vectors k_0 , k_1 , and k_T . Reflected amplitudes are then represented by A'_0 and A'_1 with associated wave vectors k'_0 and k'_1 . From Fig. 2, we see that, at the first boundary, the acoustic wave propagates into the secondary medium, now called the transition medium, and propagates a distance L before terminating into the third medium, assumed to be of infinite extent. Of interest to us then is the amplitude of the reflected wave at the first interface due to the effects of the two subsequent media.

B. Reflection Amplitude at Boundary Interfaces

We will now focus our attention on the steady-state wave propagation at the first boundary interface in Fig. 2. For an acoustical boundary, two conditions must be satisfied at all points along the boundary.⁵ First, the acoustic amplitudes on both sides of the boundary must be equal and, second, the particle velocities normal to the boundary must be equal. The first condition means that there can be no net force on the boundary plane, which implies that, along the boundary, the wave amplitude must be continuous across the interface. The second condition guarantees that the two media remain intact. Mathematically, then, the steady-state boundary conditions at the first interface are, respectively,

$$A_0 + A'_0 = A_1 + A'_1 \quad (12)$$

$$k_0(A_0 - A'_0) = k_1(A_1 - A'_1) \quad (13)$$

$$k_0 = -k'_0, \quad k_1 = -k'_1 \quad (14)$$

where, similar to k_1 , here $k_0 = n_0 \omega / c_0$.

At the second interface, A_1 has undergone a phase delay $e^{jk_1 L}$ after propagating a distance L across medium 2. Then, similar to Eqs. (12) and (13), we have the boundary conditions

$$A_1 e^{jk_1 L} + A'_1 e^{-jk_1 L} = A_T \quad (15)$$

$$k_1(A_1 e^{jk_1 L} - A'_1 e^{-jk_1 L}) = k_T A_T \quad (16)$$

where $k_T = n_T \omega / c_0$. Next, eliminating A_1 and A'_1 from Eqs. (12)–(16), we find after much straightforward algebraic manipulation that

$$1 + A'_0/A_0 = [\cos k_1 L - j(n_T/n_1) \sin k_1 L](A_T/A_0) \quad (17)$$

$$n_0 - n_0(A'_0/A_0) = (-jn_1 \sin k_1 L + n_T \cos k_1 L)(A_T/A_0) \quad (18)$$

In matrix form Eqs. (17) and (18) then become

$$\begin{bmatrix} 1 \\ n_0 \end{bmatrix} + \begin{bmatrix} 1 \\ -n_0 \end{bmatrix} \frac{A'_0}{A_0} = \begin{bmatrix} \cos k_1 L & (-j/n_1) \sin k_1 L \\ -jn_1 \sin k_1 L & \cos k_1 L \end{bmatrix} \begin{bmatrix} 1 \\ n_T \end{bmatrix} \begin{bmatrix} A_T \\ A_0 \end{bmatrix} \quad (19)$$

We now define the overall steady state wave amplitude reflection and transmission coefficients at the first boundary to be

$$r = A'_0/A_0, \quad t_r = A_T/A_0 \quad (20)$$

respectively, and we also define the trigonometric matrix of Eq. (19) to be

$$M = \begin{bmatrix} \cos k_1 L & (-j/n_1) \sin k_1 L \\ -jn_1 \sin k_1 L & \cos k_1 L \end{bmatrix} \quad (21)$$

so that Eq. (19) becomes

$$\begin{bmatrix} 1 \\ n_0 \end{bmatrix} + \begin{bmatrix} 1 \\ -n_0 \end{bmatrix} r = M \begin{bmatrix} 1 \\ n_T \end{bmatrix} t_r \quad (22)$$

We note that M is often referred to as the transfer matrix for a given layer of index n_1 and thickness L . We also note, without proof, that, in the case of N transition layers having indices $n_1, n_2, n_3, \dots, n_N$, and thickness $L_1, L_2, L_3, \dots, L_N$, respectively, the transfer matrix can be written as⁹

$$M = M_1 M_2 M_3 \cdots M_N \quad (23)$$

Equation (22) then becomes

$$\begin{bmatrix} 1 \\ n_0 \end{bmatrix} + \begin{bmatrix} 1 \\ -n_0 \end{bmatrix} r = M_1 M_2 M_3 \cdots M_N \begin{bmatrix} 1 \\ n_T \end{bmatrix} t_r \quad (24)$$

Use of the composite matrix of the form in Eq. (24) now facilitates solutions for the reflection and transmission coefficients for any number of boundary layers. In terms of matrix placeholders, Eq. (24) becomes

$$\begin{bmatrix} 1 \\ n_0 \end{bmatrix} + \begin{bmatrix} 1 \\ -n_0 \end{bmatrix} r = M_1 M_2 M_3 \cdots M_N \begin{bmatrix} 1 \\ n_T \end{bmatrix} t_r = \begin{bmatrix} A & B \\ C & D \end{bmatrix} \begin{bmatrix} 1 \\ n_T \end{bmatrix} t_r \quad (25)$$

Solving Eq. (25) for the reflection coefficients then yields the two equations

$$1 + r = At_r + n_T Bt_r \quad (26)$$

$$n_0 - n_0 r = Ct_r + n_T Dt_r \quad (27)$$

Simultaneously solving Eqs. (26) and (27) for the reflection coefficient r yields

$$r = \frac{An_0 + Bn_T n_0 - C - Dn_T}{An_0 + Bn_T n_0 + C + Dn_T} \quad (28)$$

Similarly for t_r we find

$$t_r = 2n_0/(An_0 + Bn_T n_0 + C + Dn_T) \quad (29)$$

Before proceeding, note that, whereas n_0, n_1 , and n_T are non-dispersive, the reflection and transmission coefficients are frequency dependent, as we will later show, because $k_1 = \omega n_1/c_0$. In addition, the reflected power, or reflectance, at the first interface is, in general,

$$R = |r|^2 \quad (30)$$

with the transmittance, or transmitted power, determined by

$$T = 1 - R \quad (31)$$

We note that these results are in the exact forms as those produced in the analysis of thin-film index-matching in optics.

As an example, the case of a single transition layer of length L yields a reflection coefficient of the form

$$r = \frac{n_1(1 - n_T) \cos k_1 L - j(n_T - n_1^2) \sin k_1 L}{n_1(1 + n_T) \cos k_1 L - j(n_T + n_1^2) \sin k_1 L} \quad (32)$$

Similarly, the transmission coefficient is

$$t_r = 2/[n_1(1 + n_T) \cos k_1 L - j(n_T + n_1^2) \sin k_1 L] \quad (33)$$

When Eq. (32) is parametrically investigated for various values of L, n_1 , and n_T , it can be shown that 1) there are periodic nulls and peaks in the reflection coefficient, 2) the depth and width of the periodic nulls depends on the choice of n_1 and n_T , and 3) the frequencies at which the nulls occur depend on the length of the transition region L . To continue our example, if we choose $L = \lambda_1/2$, then it can be shown that the nulls in the reflection coefficient occur at the fundamental frequency, in hertz,

$$f_0 = c_1/\lambda_1 = c_0/\lambda_0 \quad (34)$$

and periodically thereafter at each of the harmonic frequencies. Furthermore, if $L = \lambda_1/2$, then the magnitude of the reflection coefficient in Eq. (32) becomes

$$|r| = (n_T - 1)/(n_T + 1) \quad (35)$$

In particular, when $L = \lambda_1/2$, the reflection coefficient is zero when $n_T = 1$. Likewise, any desired minimum can be achieved by selecting a value for r and solving for n_T according to the relationship

$$n_T = (1 + |r|)/(1 - |r|) \quad (36)$$

III. Index-Matching for Resonance Mode Elimination

We now present an example to illustrate the process of controlling boundary reflections by means of index matching at acoustic boundary interfaces. Our example will again focus on the problem of a vibrating string, this time terminated at a rigid boundary. We will first develop the equations of motion leading to a description of the behavior of a resonantly vibrating string. We will then apply our knowledge of index matching to introduce new boundary conditions that serve to eliminate resonance behavior.

A. Equations of Motion for a Resonant String

In Fig. 3, one end of the string is fixed to a rigid boundary. The other end is attached to driving force described by Eq. (4). The transverse force in newtons per meter due to string tension τ is described by

$$F_\tau = \tau \frac{\partial^2 y}{\partial x^2} \quad (37)$$

whereas the force in newtons per meter due to acceleration of the string mass is given as

$$F_a = \rho_s \frac{\partial^2 y}{\partial t^2} \quad (38)$$

where ρ_s is the mass density of the string in kilograms per meter.

A damping force also exists that is the result of the elastic properties of the string. This elastic resistance to the string's movement is a mechanical resistance R_d distributed across the length of the string. The magnitude of the resistance is related to mass density and is also velocity dependent.¹⁰ The damping force in newtons per meter resulting from this resistance can be represented by

$$F_{\text{damp}} = R_d \frac{\partial y}{\partial t} \quad (39)$$

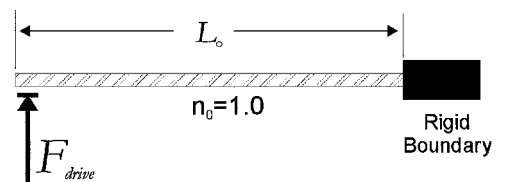


Fig. 3 Forced string with rigid boundary.

By inspection, the units for R_d must be newton seconds per square meter. Incorporating these forces into the equation of motion for the string, we now have

$$F_{\text{drive}} + F_{\tau} = F_a + F_{\text{damp}} \quad (40)$$

or

$$\tau \frac{\partial^2 y}{\partial x^2} - \rho_s \frac{\partial^2 y}{\partial t^2} - R_d \frac{\partial y}{\partial t} = -F \cdot e^{j\omega t} \quad (41)$$

If we assume a steady-state solution of the form

$$y(x, t) = \psi(x) e^{j\omega t} \quad (42)$$

then Eq. (41) becomes

$$\frac{\partial^2 \psi}{\partial x^2} + \frac{\omega^2}{c_0^2} \psi e^{j\omega t} - j \frac{\omega R_d}{\tau} \psi e^{j\omega t} = -\frac{F}{\tau} e^{j\omega t} \quad (43)$$

Rearranging terms and dividing by $e^{j\omega t}$, we find that

$$\frac{\partial^2 \psi}{\partial x^2} + \left(\frac{\omega^2}{c_0^2} - j \frac{\omega R_d}{\tau} \right) \psi = -\frac{F}{\tau} \quad (44)$$

We now let

$$\gamma^2 = \omega^2 / c_0^2 - j(\omega R_d / \tau) \quad (45)$$

so that Eq. (44) becomes

$$\frac{\partial^2 \psi}{\partial x^2} + \gamma^2 \psi = \frac{-F}{\tau} \quad (46)$$

The complete solution to the second-order differential equation of Eq. (46) is obtained from the sum of the general and particular solutions.¹¹ The result is

$$\psi = C \sin(\gamma x) - F / \tau \gamma^2 \quad (47)$$

with amplitude C being determined by boundary conditions. Specifically, at $x = L_0$, $\psi = 0$, so that

$$C = F / \tau \gamma^2 \sin(\gamma L_0) \quad (48)$$

When the temporal dependence is ignored, the amplitude of the displacement at any position along the string is then

$$\psi = \frac{F}{\tau \gamma^2} \left[\frac{\sin(\gamma x) - \sin(\gamma L_0)}{\sin(\gamma L_0)} \right] \quad (49)$$

Notice that, if the damping force was absent, that is, if $R_d = 0$, then the displacement would become infinite in Eq. (49) at resonance frequencies ω_r given as

$$\omega_r = m \pi c_0 / L_0 \quad (50)$$

or

$$f_r = m c_0 / 2 L_0 \quad (51)$$

where $m = 1, 2, 3, \dots$ and $f_r = \omega_r / 2\pi$. When the damping force is present ($R_d > 0$), the imaginary term in Eq. (45) ensures that resonances are bounded. In essence, the damping coefficient R_d principally governs the amplitude of the resonance displacement.

As a case study, we can analyze the resonance behavior for a string having the arbitrary physical parameters in Table 1. The fundamental resonance frequency in hertz for this case is

$$f_0 = c_0 / 2 L_0 = \sqrt{\tau / \rho_s} \cdot 1 / 2 L_0 = 63.25 \quad (52)$$

with harmonic frequencies identified by

$$f_{m-1} = m f_0 \quad (m = 2, 3, \dots) \quad (53)$$

For our analysis, we will only concern ourselves with the peak value of the magnitude of the complex string displacement amplitude at any given frequency, over the range $0 \leq x \leq L_0$. This is given by

$$\psi_{\text{peak}} = \max \left\{ \left| \frac{F}{\tau \gamma^2} \left[\frac{\sin(\gamma x) - \sin(\gamma L_0)}{\sin(\gamma L_0)} \right] \right| \right\}_{x=0}^{x=L_0} \quad (54)$$

Figure 4 shows the peak string displacement as a function of excitation frequency for the elastic damped case represented in Table 1. The fundamental frequency can clearly be identified, as can the first and second harmonics ($m = 2$ and 3).

B. Index-Matching for Resonance Elimination

The developed principles for acoustic index matching can now be applied to reduce or eliminate energy in the fundamental and harmonic frequency resonances observed in Fig. 4. To accomplish this goal, we will utilize our earlier developed theory for single transition layer boundaries to our string problem. We now insert index-matching layers between the string launch medium and the terminating boundary as shown in Fig. 5. A rigid boundary following the terminating layer is maintained to preserve our original steady-state description of the vibrating string. The existence of the

Table 1 Forced string parameters

| Description | Parameter | Value |
|-----------------------|-----------|---------------------------|
| Peak driving force | F | 0.1 N/m |
| String length | L_0 | 50 cm |
| String tension | τ | 2 N |
| Mass density | ρ_s | 0.0005 kg/m |
| Mechanical resistance | R_d | 0.01 N · s/m ² |

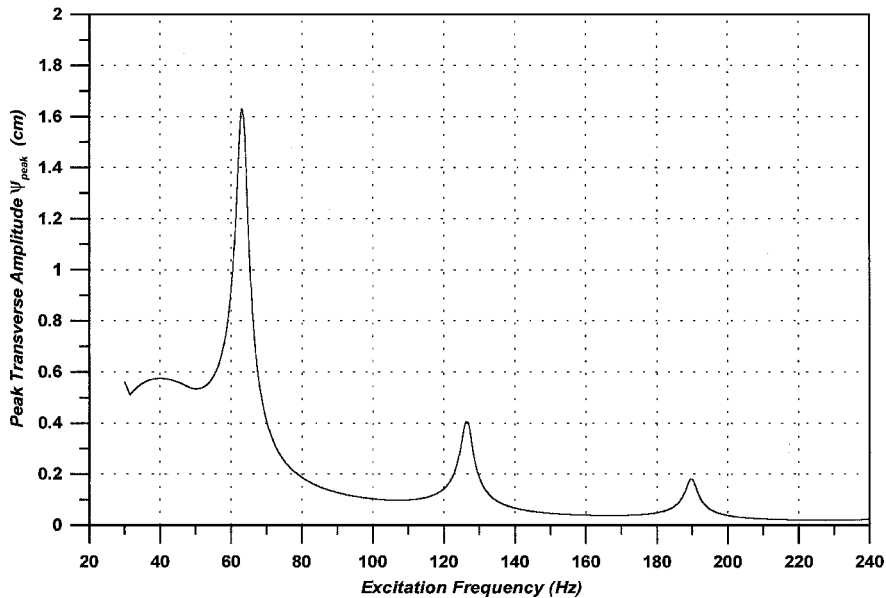


Fig. 4 Displacement response for forced string with elastic damping, theoretical analysis with elastic damping.

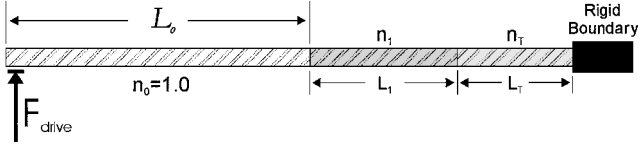


Fig. 5 Single transition layer index matching applied to a forced string.

rigid boundary does not present a problem. Under steady-state conditions, all frequency components normally propagate into a hard boundary. In our following design, frequency components away from the resonant frequency propagate a length L_0 and terminate at the (n_0, n_1) boundary, whereas normally resonant frequencies will propagate through the index-matching layers and terminate at the rigid boundary. Notice that terminal layer may be of any arbitrary length, as long as the total propagation length $L_0 + L_1 + L_T$ is not a multiple of the resonant frequency's wavelength. Otherwise another resonant geometry would exist, confounding the effect of our resonance reduction technique.

Choosing the appropriate indices to optimize the desired response for specified in-band and out-of-band reflectance is the subject of numerous texts.^{12–19} In fact, closed-form solutions of Eq. (28) needed to predict the exact index values for resonance suppression are not obtainable for the cases of two or more transition boundary layers. Many analytical methods and computer codes exist to aid the designer in choosing materials and boundary geometries for optical filter designs. These same tools are applicable in the acoustical domain. Of the methods available, we chose a merit function approach for selecting the appropriate values for acoustic indices and boundary layer dimensions for this example.

A quadratic merit function (MF) based on a quadratic sum of differences was constructed of the form

$$MF = \sqrt{(A_{\text{desired}} - A_{\text{achieved}})^2 + (B_{\text{desired}} - B_{\text{achieved}})^2 + \dots} \quad (55)$$

where the subscripted MFs A, B, \dots represent the desired and obtained characteristics of the computer-modeled response. Use of the quadratic MF allows convergence of numerical computations involving numerous parameters. Clearly, the value of the MF ideally approaches zero as desired and achieved responses grow closer in agreement.

In pursuit of the optimized index values, several features of the resonant response in Fig. 4 were analyzed, and the behavior necessary to correct the response became the desired features of the MF. The amplitude at the fundamental resonance amplitude, for example, needs to be reduced to bring the response in line with the nonresonant frequency rolloff. We define the required amplitude reduction at the fundamental resonance frequency to be A_F .

In addition, the sharpness of the resonant amplitude response should be a good match to that of the resonance peak without affecting the response at nonresonance frequencies. We quantify this characteristic with the parameter Q , defined as

$$Q = \frac{\text{bandwidth}}{\text{center frequency}} \quad (56)$$

where the bandwidth is measured at the 50% maximum points on the response of the resonance peaks.

Although not directly a factor of the MF, a periodic response is also warranted for the elimination of harmonic frequencies. The desired periodic response of the applied boundary might require different amplitudes at the fundamental and first harmonic frequencies. Therefore, we independently define the desired attenuation of the first-order harmonic amplitude to be A_H .

Finally, we desire that overall loss for nonresonant frequencies be as low as possible, to not eliminate the response all together. In essence, we would prefer the overall gain of the response to be close to unity. Therefore, we defined the third merit factor to be A_G , where the amplitude measurement for gain determination was performed in a region between the resonance peaks.

Using these four parameters to describe the preferred performance, the following figure of merit can now be defined based on Eq. (55):

Table 2 Target merit values for string resonance reduction

| Parameter | Factor | Value |
|-------------------------|--------|-------|
| Fundamental attenuation | A_F | 4.92 |
| Harmonic attenuation | A_H | 4.92 |
| Nonresonant gain | A_G | 0.9 |
| Q | Q | 0.17 |

$$MF = \sqrt{(A_F - A'_F)^2 + (Q - Q')^2 + (A_H - A'_H)^2 + (A_G - A'_G)^2} \quad (57)$$

where the primed terms in Eq. (57) refer to the computed values of the desired parameters. As the computed values begin to approach the desired values, each term in the quadratic vanishes. It follows then that the figure of merit for our indices selection will be optimized when MF is made as small as possible.

Values for the desired merit factors selected for resonance reduction were obtained by inspection of the string response in Fig. 4 and are summarized in Table 2. In essence, the desired merit factors describe the antiresponse for the index-matched boundary. After optimization, when multiplied by the resonance response of Fig. 4, the reflection coefficient of Eq. (32) should result in a displacement response void of resonance peaks.

We recall from our earlier discussions that a boundary layer of length $L_1 = \lambda_1/2$ produces nulls in the reflection coefficient at the fundamental frequency and periodically thereafter at each of the harmonic frequencies. This periodicity corresponds exactly with the periodicity of our string resonance peaks. Therefore, we will choose $L_1 = \lambda_1/2$ to be our boundary dimension. Furthermore, we can utilize the form of the reflection coefficient in Eq. (35) to predetermine the optimum value for the terminal index value. From the required fundamental attenuation factor, and nonresonant gain, the minimum reflection amplitude needs to be

$$r_{\min} = A_G/A_F = 0.183 \quad (58)$$

Now from Eq. (35), the optimum terminal index value is computed to be $n_T = 1.45$. Because we have assumed all media to be lossless, this result could eliminate the two terms of our quadratic MF, A_F and A_H , and allow us to optimize the remaining terms through manipulation of n_1 . We will instead perform our merit search based on the full compliment of merit factors and compare our results for n_T to our predetermined value.

The MF of Eq. (57) was implemented using MATLAB® and run using the values in Table 2. The analysis was for a single transition layer index-matching boundary modeled with a $\lambda_1/2$ boundary region length based on a center frequency of 63.25 Hz, where λ is the wavelength of the acoustic wave in each corresponding region. Boundary reflectance was computed using Eq. (32) over the frequency range of interest, which included the fundamental and resonance frequencies. The software then computed actual merit factors from the features of each reflectance curve and applied them to the quadratic MF. Index values for n_1 and n_T were incremented between 1.00 and 10.00. Because zero merit values were not likely, a threshold of $MF < 0.2$ was applied to the merit computation, which sifted out promising refractive indices combinations. From the sifted list, specific indices combinations were hand picked for inspection. The search produced an optimum result for index values of $n_0 = 1.0$, $n_1 = 5.39$, and $n_T = 1.45$, where using Eqs. (9), (11), and (50), we also find that the required transition layer length in centimeters is

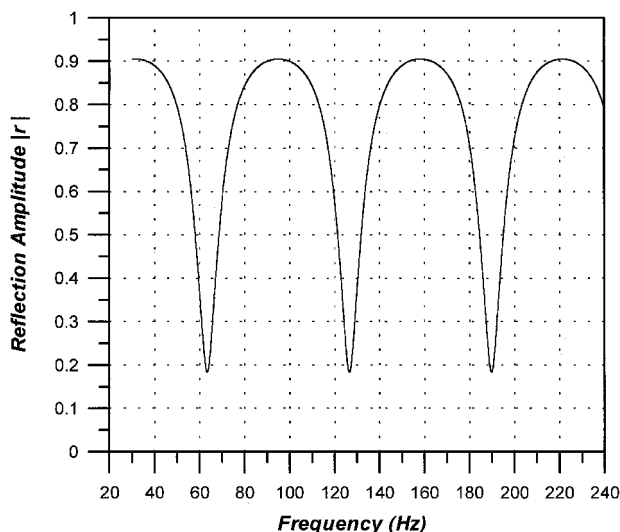
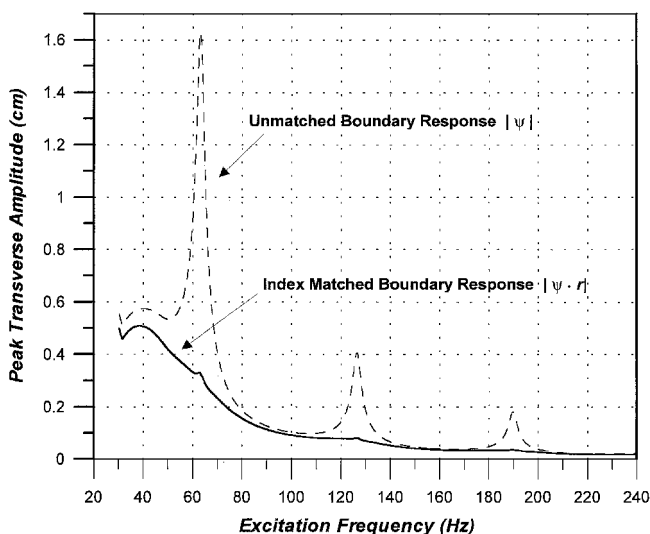
$$\lambda_1/2 = L_0/n_1 = 9.28 \quad (59)$$

Table 3 summarizes the merit factors produced for the optimum case. We note that the merit search produced the same value for the terminal index ($n_T = 1.45$) as that produced from the prediction of Eq. (35). Figure 6 shows the magnitude of the reflection coefficient for this candidate case.

By applying the boundary geometry to the string that produced the response in Fig. 4, we can see the benefit obtained in resonance reduction. The final amplitude response was obtained by multiplying the complex amplitude of resonant string displacement ψ and the

Table 3 Merit factors representing optimum MF search

| Parameter | Factor | Target value | Obtained value | % Difference |
|-------------------------|--------|--------------|----------------|--------------|
| Fundamental attenuation | A_F | 4.92 | 4.93 | 1.0 |
| Harmonic attenuation | A_H | 4.92 | 4.93 | 1.0 |
| Nonresonant gain | A_G | 0.9 | 0.905 | 0.5 |
| Q | Q | 0.17 | 0.19 | 2.0 |
| MF | MF | 0 | 0.042 | — |

**Fig. 6** Single transition layer response based on optimized figure of merit for correction of string model with elastic damping, $\lambda/2$ boundary length, $n_0 = 1.0$, $n_1 = 5.39$, and $n_T = 1.45$.**Fig. 7** Average displacement response for forced string with elastic damping, index matched response.

complex reflection amplitude r . The final magnitude of this product was plotted in Fig. 7, which shows the response along with the original unmatched resonant response. The resulting behavior is one void of the resonance peaks.

A single transition layer, index-matching boundary was sufficient to eliminate resonances in our forced string example. Because all media is assumed to be lossless, this resulted in the condition that the required attenuation of the fundamental and first harmonic frequencies were equal. Had the problem required different attenuation values at these frequencies, two-boundary layers would have been required to control the fundamental and harmonic nulls of the re-

flection amplitudes independently. With enough layers, and enough insights into behavioral trends, nearly any response can be emulated.

IV. Conclusions

The results of this theoretical study illustrate that resonance reduction can be realized for transverse wave propagation in acoustical structures, utilizing the concept of optical index of refraction as applied to boundary interfaces. A principle benefit of the index-matching approach is that conventional analysis and design tools available for the design of optical thin-film coatings have utility in the design of acoustical boundaries involving transverse acoustic waves. In contrast to traditional damping techniques, index matching allows specific frequencies to be emphasized or deemphasized without disturbing the frequency response at other frequencies of interest. In the cited example, string resonances were eliminated while maintaining reflection at the boundary for all other frequencies. Theoretically, through proper manipulation of boundary geometries and material mass densities, the acoustical transmission and reflection at the boundary can be tailored for any desired response. Applications that could benefit from index-matching methods for control of boundary response include adaptive mirror design, self-deploying space mirrors, electrostatic loudspeakers, and ultrasonics. The U.S. Air Force Research Laboratories have successfully used the described techniques in the elimination of resonance in metalized mirror structures used in the optical simulation of atmospheric turbulence. The theory should also have application to beams and membranes because as the extension of the theory to two-dimensional structures can easily be made.

References

- ¹Furman, S., and Tikhonravov, A. V., *Basics of Optics of Multilayer Systems*, Editions Frontiers, Gif-sur-Yvette, France, 1992.
- ²Fowles, G. R., *Introduction to Modern Optics*, Dover, New York, 1975, pp. 4, 5.
- ³Born, M., and Wolf, E., *Principles of Optics*, Pergamon, New York, 1975, pp. 13, 14.
- ⁴Maleki, I., *Physical Foundations of Acoustics*, Pergamon, Warsaw, 1969, pp. 83–85 (translation).
- ⁵Kinsler, L. E., Frey, A. R., Coppens, A. B., and Sanders, J. V., *Fundamentals of Acoustics*, Wiley, New York, 1982, pp. 124, 125.
- ⁶Kinsler, L. E., Frey, A. R., Coppens, A. B., and Sanders, J. V., *Fundamentals of Acoustics*, Wiley, New York, 1982, p. 30.
- ⁷Kinsler, L. E., Frey, A. R., Coppens, A. B., and Sanders, J. V., *Fundamentals of Acoustics*, Wiley, New York, 1982, pp. 36–55.
- ⁸French, A. P., *Vibrations and Waves*, W. W. Norton, New York, 1971, p. 207.
- ⁹Born, M., and Wolf, E., *Principles of Optics*, Pergamon, New York, 1975, pp. 57, 58.
- ¹⁰Kinsler, L. E., Frey, A. R., Coppens, A. B., and Sanders, J. V., *Fundamentals of Acoustics*, Wiley, New York, 1982, p. 91.
- ¹¹Braun, M., *Differential Equations and Their Applications*, Springer-Verlag, New York, 1978, pp. 76–104.
- ¹²Tikhonravov, A. V., and Dobrowolowski, J. A., "Quasi-Optimal Synthesis for Anti-Reflection Coatings: A New Method," *Applied Optics*, Vol. 32, No. 22, 1993, pp. 4265–4275.
- ¹³Cox, J. T., and Hass, G., "Antireflection Coatings for Optical and Infrared Optical Materials," *Physics of Thin Films*, Academic Press, New York, 1964, pp. 239–304.
- ¹⁴Mussett, A., and Thelen, A., "Multilayer Antireflection Coatings," *Progress in Optics*, Pergamon, New York, 1970, pp. 203–237.
- ¹⁵Kard, P. G., *Analysis and Synthesis of Multilayer Interference Coatings*, Vlagus, Tallin, Estonia, 1971.
- ¹⁶Knittl, Z., *Optics of Thin Films*, Wiley, New York, 1976.
- ¹⁷Macleod, H. A., *Thin Film Optical Filters*, McGraw-Hill, New York, 1986.
- ¹⁸Thelen, A., *Design of Optical Interference Coatings*, McGraw-Hill, New York, 1988.
- ¹⁹Furman, S., and Tikhonravov, A. V., *Basics of Optics of Multilayer Systems*, Editions Frontiers, Gif-sur-Yvette, France, 1992.

W. J. Devenport
Associate Editor